Molecular Cancer Therapeutics

A novel temozolomide-perillyl alcohol conjugate exhibits superior activity against breast cancer cells in vitro and intracranial triple-negative tumor growth in vivo

Thomas C Chen, Hee-Yeon Cho, Weijun Wang, et al.

Mol Cancer Ther Published OnlineFirst March 12, 2014.

Author Manuscript Published OnlineFirst on March 12, 2014; DOI: 10.1158/1535-7163.MCT-13-0882
Author manuscripts have been peer reviewed and accepted for publication but have not yet been edited.

A novel temozolomide-perillyl alcohol conjugate exhibits superior activity against breast cancer cells in vitro and intracranial triple-negative tumor growth in vivo

Thomas C. Chen[1,2], Hee-Yeon Cho[2], Weijun Wang[1], Manasi Barath[3], Natasha Sharma[4], Florence M. Hofman[2], Axel H. Schönthal[3]

Authors' Affiliation: Departments of [1]Neurosurgery, [2]Pathology, [3]Molecular Microbiology and Immunology, [4]Pharmaceutical Sciences; University of Southern California, Los Angeles, California, USA.

Corresponding authors: Axel H. Schönthal, University of Southern California, 2011 Zonal Avenue, HMR-405, Los Angeles, CA 90089. Phone: 323-442-1730; Fax: 323-442-1721; E-mail: schontha@usc.edu. Thomas C. Chen, University of Southern California, 2011 Zonal Avenue, Los Angeles, CA 90089. Phone: 323-442-3918; Fax: 323-442-3049; E-mail: tcchen@usc.edu

Running title: Novel temozolomide analog for intracranial breast cancer

Key words: blood-brain-barrier; drug half-life; intracranial metastases.

Abbreviations list: GBM: glioblastoma multiforme; MGMT: O6-methylguanine-DNA methyltransferase; O6-BG: O6-benzylguanine; POH: perillyl alcohol; TMZ: temozolomide; T-P: perillyl alcohol covalently linked to temozolomide.

Financial Support

This work was supported by funds provided by The Regents of the University of California, California Breast Cancer Research Program, Grant Number No 19IB-0141, to T.C. Chen and

A.H. Schönthal. The opinions, findings, and conclusions herein are those of the authors and not necessarily represent those of The Regents of the University of California, or any of its programs. We also acknowledge the James Hale Family for generous research support (to T.C. Chen).

ABSTRACT

There is no effective therapy for breast cancer that has spread to the brain. A major roadblock is the blood-brain-barrier (BBB), which prevents the usual breast cancer drugs from effectively reaching intracranial metastases. The alkylating agent temozolomide (TMZ) is able to penetrate the BBB and has become the gold standard for chemotherapeutic treatment of glioblastoma. However, when it was tested in clinical trials for activity against brain metastases of breast cancer, the results were mixed and ranged from “encouraging activity” to “no objective responses.” In an effort to generate an agent with greater activity against intracranial breast metastases, we synthesized a TMZ analog where the natural product perillyl alcohol (POH) was covalently linked to TMZ’s amide functionality. The resulting novel compound, called TMZ-POH (T-P), displayed greatly increased anticancer activity in a variety of breast cancer cell lines, inclusive of TMZ-resistant ones. It caused DNA damage and cell death much more efficiently than its parental compound TMZ, because linkage with POH increased its biological half-life and thus provided greater opportunity for placement of cytotoxic DNA lesions. In an intracranial mouse tumor model with triple-negative breast cancer, T-P revealed considerably greater therapeutic efficacy than TMZ, where a single cycle of treatment extended median survival benefit from 6 days (in the case of TMZ) to 28 days. At the same time, T-P appeared to be well tolerated by the animals. Thus, T-P may have potential as a novel therapy for brain-targeted breast cancer metastases.

1. Introduction

There is no effective therapy for breast cancer that has spread to the brain. This therapeutic challenge once was a late aspect of disease progression, but increasingly is becoming a first site of disease progression after otherwise successful treatment of primary tumor and metastases outside the cranium (1). Current therapeutic approaches consist of surgery, radiation, and chemotherapy. Chemotherapy is obstructed by the inability of most chemotherapeutic agents to effectively penetrate the blood brain barrier. For example, traditional breast cancer therapeutics, such as paclitaxel or doxorubicin, only reach brain metastases at concentrations that are far lower than needed to be therapeutically active (2).

The alkylating agent temozolomide (TMZ) is able to cross the BBB after oral dosing and has become the chemotherapeutic standard of care for patients with glioblastoma multiforme (GBM) (3). However, when TMZ was tested for activity against brain metastatic breast cancer in heavily pretreated patients, it revealed mixed outcomes that ranged from “encouraging activity” and “disease control” to “well-tolerated, but no objective responses” (4-9). The underlying basis for these inconsistent results was not investigated, but it is conceivable that these differences may have been due to variable expression levels of O6-methylguanine-DNA methyltransferase (MGMT; also called O6-alkylguanine-DNA alkyltransferase, AGT), a DNA repair enzyme that removes alkyl groups located on the O6-position of guanine (10, 11). Because the primary toxic DNA lesion set by TMZ is alkylation of O6-guanine, high expression levels of MGMT protect tumor cells from the cytotoxic impact of TMZ and provide treatment resistance (12, 13). When MGMT expression was investigated in breast cancer metastases to the brain, it was found that over half of the intracranial lesions analyzed were strongly positive for MGMT immunoreactivity (14). It is therefore conceivable that improved outcomes of TMZ treatment might be achievable if patients with brain metastatic breast cancer were stratified according to MGMT expression levels prior to the onset of chemotherapy.

MGMT activity is unusual in that it represents a “suicide” mechanism, whereby acceptance of the alkyl group from DNA irreversibly inactivates the enzyme and leads to its rapid degradation (10). This feature is exploited by the use of specific MGMT inhibitors, such as O6-benzylguanine (O6-BG), which act as pseudosubstrates (15). Benzylation of MGMT via reaction with O6-BG causes the same structural change in the enzyme as that seen after alkylation following DNA repair, and therefore also leads to rapid degradation of the protein (16). Ablation of MGMT activity after treatment of MGMT-positive cells with O6-BG generally increases their sensitivity to killing by TMZ, and this has been well established in numerous in vitro and in vivo tumor models (see detailed refs. in (12, 17)). However, a recent phase-II clinical trial yielded mixed outcomes when O6-BG and TMZ were administered to brain cancer patients with TMZ-resistant tumors: while the addition of the MGMT inhibitor restored TMZ-sensitivity in a fraction (16%) of patients with anaplastic glioma, there was no significant effect (3%) in patients with GBM (18). While the underlying reasons for this disappointing outcome remain to be established, the limited response documented in this trial does not generate enthusiasm for the potential study of this drug combination in brain metastatic breast cancer patients. As an alternative, we focused our research on efforts to improve the anticancer activity of TMZ itself.

POH is a monoterpene isolated from the essential oils of several plants and fruits, such as peppermint, spearmint, cherries and celery seeds (19). Although this compound had shown promising activity in several preclinical cancer models (20, 21), it did not enter clinical practice, primarily because dose-limiting intestinal toxicity became evident in clinical trials (22-24). However, recent phase I/II clinical studies in Brazil demonstrated that simple intranasal inhalation of POH was effective against recurrent GBM, in the absence of detectable toxic events (25, 26). Based on these promising results, we hypothesized that covalently linking POH to TMZ might result in a novel therapeutic agent with superior activity against intracranial tumors. Here, we present our results validating this prediction in various breast cancer cell lines in vitro and in vivo.

2. Materials and Methods

2.1. Pharmacological agents

TMZ was obtained from the pharmacy at the University of Southern California (USC) and dissolved in ethanol to a concentration of 50 mM. T-P was provided by NeOnc Technologies (Woodland Hills, CA) and was dissolved in DMSO at 100 mM. POH and O6-BG were purchased from Sigma-Aldrich (St. Louis, MO) and diluted with DMSO to make stock solutions of 100 mM. DMSO was from Sigma-Aldrich. In all cases of cell treatment, the final DMSO concentration in the culture medium never exceeded 0.5%. Stock solutions of all drugs were stored at –20˚C.

2.2. Cell lines

Several of the human breast cancer cell lines were obtained from the American Tissue Culture Collection (ATCC; Manassas, VA), and these cells were passaged for less than 6 months in our laboratory after receipt or resuscitation. HCC-1937 cells were provided by Michael F. Press (USC). The brain-seeking line MDA-MB-231-br (originally described by Yoneda et al. (27)) was obtained from Steve Swenson (USC). These latter two lines were not authenticated by the authors. Cells were propagated in DMEM (provided by the Cell Culture Core Lab of the USC/Norris Comprehensive Cancer Center and prepared with raw materials from Cellgro/MediaTech, Manassas, VA) supplemented with 10% fetal bovine serum, 100 U/mL penicillin, and 0.1 mg/mL streptomycin in a humidified incubator at 37°C and a 5% CO_2 atmosphere.

2.3. Colony formation assay

Depending on the cell line (and plating efficiency), 200-350 cells were seeded into each well of a 6-well plate. After cells had fully attached to the surface of the culture plate, they were exposed to drug treatment (or DMSO solvent alone) for various times up to 48 hours. Thereafter, the drugs were removed, fresh growth medium was added, and the cells were kept in culture undisturbed for 12–16 days, during which time the surviving cells spawned colonies of

descendants. Colonies (defined as groups of >50 cells) were visualized by staining for 4 hours with 1% methylene blue (in methanol), and then were counted.

In the case of O6-BG treatment, cells were pretreated with 10 μM O6-BG for one hour before addition of TMZ or T-P. After 24 hours, another 10 μM O6-BG was added to the medium. Another 24 hours later, drug-laced medium was removed, and fresh medium without drugs was added. Thereafter, cells remained undisturbed until staining with methylene blue (1% in methanol).

2.4. Stable transfections

MDA-MB-231 cells were co-transfected in 6-well plates with the use of Lipofectamine 2000 (Invitrogen, Carlsbad, CA) according to manufacturer's instructions. We combined 2 μg pSV2MGMT (containing the human MGMT cDNA) with 0.2 μg pSV2neo (containing the neomycin gene for selection of cells in G418). Both plasmids were kindly provided by Bernd Kaina (Mainz, Germany) (28). Individual clones of transfected cells were selected in medium containing 750 μg/mL G418 and propagated in 250 μg/mL G418. G418 was obtained as G418 disulfate salt from Sigma-Aldrich and dissolved in PBS at 75 mg/mL. Selection medium was removed from cells several days before experimental drug treatment.

2.5. Immunoblots

Total cell lysates were analyzed by Western blot analysis as described earlier (29). The primary antibodies were purchased from Cell Signaling Technology (Beverly, MA) or Santa Cruz Biotechnology, Inc. (Santa Cruz, CA) and used according to the manufacturers' recommendations. All immunoblots were repeated at least once to confirm the results.

2.6. In vivo model

All animal protocols were approved by the Institutional Animal Care and Use Committee (IACUC) of USC, and all rules and regulations were followed during experimentation on animals. Athymic mice (Harlan, Inc., Indianapolis, IN) were implanted intracranially with $2x10^5$ cells, as previously described (30). We used a subline of MDA-MB-231 cells called D3H2LN,

which was transfected with the firefly luciferase gene and had been selected for aggressive growth and metastasis in vivo (31). Ten days after intracranial implantation, efficient tumor take was confirmed in all animals via non-invasive whole-body bioluminescent imaging. For this purpose, mice were intravenously injected with 50 mg/kg D-Luciferin (Perkin Elmer, Waltham, MA) and imaged using the Xenogen IVIS-200 Imaging System (Caliper/Perkin Elmer). Images were analyzed by region-of-interest (ROI) analysis using the Living Image software package (Caliper/Perkin Elmer) to quantitate light output (radiance, i.e., photons per second per square centimeter per steradian).

Animals were distributed into three groups of 8 animals each, so that each group contained animals with comparable radiance within the ROI (i.e., area of the head) and drug treatment was initiated. Group 1 was the control group that received vehicle only (45% glycerol, 45% ethanol, 10% DMSO) via subcutaneous injection. Group 2 was the experimental group that received 25 mg/kg T-P via subcutaneous (s.c.) injection. Group 3 was the comparison group and animals received 25 mg/kg TMZ via gavage. (Because the bioavailability of TMZ essentially is 100% when given orally (32) (and cannot be further increased via s.c. or i.v. delivery (33)), we preferred the well-established, most frequently used administration of TMZ via oral gavage; in the case of T-P, however, bioavailability data is lacking, and therefore we decided to administer this compound via s.c. injection.) Treatment was once per day for a period of 10 days (i.e., 10 treatments total). Thereafter, all surviving animals were imaged again, once per week.

2.7. Statistical analysis

All parametric data were analyzed using the Student t-test to calculate the significance values. The survival distributions in the Kaplan-Meier plot were analyzed with the non-parametric Wilcoxon test. A probability value (p) <0.05 was considered statistically significant.

3. Results

A novel analog of temozolomide (TMZ) was created by covalently linking perillyl alcohol

(POH) to TMZ's amide functionality (***Suppl. Fig. S1***). The cytotoxic potency of this new compound, T-P, was analyzed by colony formation assay (CFA) in a variety of human breast cancer cell lines and compared to the cytotoxicity of TMZ. We used estrogen receptor positive cells MCF7 and T47D, the triple-negative lines MDA-MB-231, MDA-MB-468, and HCC-1937, and a brain-seeking variant of the 231 cell line, MDA-MB-231-br. As shown in ***Fig. 1A***, low micromolar concentrations of T-P prevented colony formation in all six cell lines, and in all instances T-P's potency was substantially stronger than that of TMZ.

Previous studies showed that POH is able to exert cytotoxic effects in cancer cells, although concentrations approaching the millimolar range were required (34, 35). We therefore tested whether simply mixing the two compounds TMZ and POH could mimic the effects of the T-P conjugate. MDA-MB-231 cells were treated with the individual compounds (T-P, TMZ or POH) alone, or with an equimolar mix of TMZ plus POH, and cell survival was analyzed by CFA. As shown in ***Fig. 1B***, T-P was much more potent than a mix of TMZ plus POH, i.e., mixing TMZ with POH was unable to achieve the strong cytotoxic potency of T-P, and in fact, the addition of equimolar concentrations of POH to TMZ did not increase the potency over TMZ alone. For instance, 10 μM TMZ reduced colony formation by about 50%, and the combination of 10 μM TMZ with 10 μM POH also caused a 50% reduction; in comparison, 10 μM T-P caused about 95% fewer colonies (a photo of a representative CFA is shown in ***Suppl. Fig. S2***). Consistent with earlier reports, POH by itself required concentrations well above 100 μM in order to become cytotoxic, and its IC50 in MDA-MB-231 cells was about 700 μM (***Fig. 1A***). Thus, an equimolar mix of TMZ plus POH was unable to mimic the strong cytotoxic potency of the T-P conjugate, and this was confirmed in several additional cell lines tested. Altogether, these results present T-P as a novel compound with increased potency over TMZ that cannot be matched by merely mixing its individual parts, TMZ and POH, and this outcome was confirmed in several additional cell lines tested, including the brain-tropic variant of MDA-MB-231.

Because the DNA repair protein MGMT is known to play a key role in cellular resistance to

TMZ, we next investigated how it would impact the cytotoxic potency of T-P. We first determined its basal level of expression in the six breast cancer cell lines we used above. ***Fig. 2A*** shows that three cell lines (MDA-MB-468, HCC-1937, MCF7) were strongly positive, whereas the others (T47D, MDA-MB-231, MDA-MB-231-br) had undetectable levels of MGMT protein, as determined by Western blot analysis. For comparison purposes, we also assessed MGMT protein levels in three commonly used GBM cell lines known to be MGMT negative (U251, LN229) and positive (T98G). This side-by-side evaluation revealed that MGMT protein levels in the positive breast cancer lines were similar to the levels found in the T98G brain cancer line (***Fig. 2B***).

We next aligned MGMT expression with the cytotoxic potency of T-P in comparison to TMZ. As summarized in ***Table 1***, the IC50 of T-P (i.e., the concentration required to decrease colony formation by 50%) was noticeably higher in all three MGMT-positive breast cancer cell lines. Whereas the IC50 in MGMT-negative cell lines ranged from 1.2 to 4.6 μM, it increased to 31 to 33 μM in the three MGMT-positive lines. Nonetheless, these IC50 values still were substantially lower than the corresponding IC50s of TMZ for each cell line. Noteworthy as well is the differential (fold increase in potency) between T-P and TMZ shown in ***Table 1***: The fold-increase in cytotoxic potency of T-P, as compared to TMZ, is consistently greater in each of the MGMT-positive cell lines (6.3 to 15.5-fold) as compared to the MGMT-negative cell lines (3.2 to 4.3-fold). This latter finding suggests that the increased potency of T-P over TMZ, although apparent in all cell lines analyzed, might become particularly advantageous in the context of therapeutically targeting MGMT-positive cells.

We further characterized the relevance of MGMT in T-P's cytotoxic effects, in comparison to TMZ. The major cytotoxic DNA lesion set by TMZ is methylation of O6-guanine, and it is well known that removal of this methyl group by MGMT leads to rapid degradation of the DNA repair protein. As well, the pseudosubstrate O6-BG also activates the suicide mechanism of MGMT, which is confirmed in ***Fig. 2C***, showing that treatment of cells with O6-BG strongly decreases

MGMT protein levels. Treatment of cells with TMZ also down-regulates MGMT levels, but the effect is fairly weak and high concentrations of the drug are required. In comparison, T-P affects MGMT levels more potently than TMZ; for instance, while 50 μM TMZ has no effect, 50 μM T-P causes a significant decrease (***Fig. 2C***). Together, these results indicate that T-P's superior potency over TMZ may involve more extensive methylation of O6-guanine targets.

While the above results suggested that T-P's mechanism of action perhaps was due to the drug's increased efficacy of setting cytotoxic DNA lesions, there was also a possibility that covalently conjugating POH might have conferred additional mechanistic features to the new molecule. We therefore performed additional experiments to characterize the significance of DNA damage, and in particular O6-guanine methylation, caused by T-P.

While the experiments summarized in ***Table 1*** revealed a correlation of MGMT positivity with decreased T-P toxicity, they did not establish cause and effect. To investigate the latter, we stably transfected MGMT-negative MDA-MB-231 cells with MGMT cDNA and isolated individual clones. ***Fig. 3A*** shows elevated expression of MGMT protein in two different clones (231-MGMT-1 and 231-MGMT-2) of transfected cells. Both clones were treated with increasing concentrations of T-P and TMZ and analyzed by CFA. As shown in ***Fig. 3B*** (and summarized in ***Suppl. Table S1***), resistance of cells to drug treatment clearly increased for both T-P and TMZ, as compared to parental cells. Intriguingly however, similar to what was noted in ***Table 1***, resistance to T-P increased less than resistance to TMZ (***Suppl. Table S1***).

CFAs were also performed with the inclusion of the MGMT inhibitor O6-BG. Cells were pre-treated with O6-BG before addition of T-P or TMZ. As shown in ***Fig. 4A***, O6-BG had no effect on the survival of drug-treated MDA-MB-231 cells, consistent with their MGMT-negative status that does not provide a target for O6-BG. In contrast, O6-BG greatly enhanced toxicity of T-P and TMZ in 231-MGMT-1 (***Fig. 4B***) and 231-MGMT-2 cells (not shown***)***. Similarly, O6-BG also increased the cytotoxic outcome of T-P and TMZ treatment in MGMT-positive MDA-MB-468 (***Fig. 4C***) and MCF7 cells (not shown). Altogether, these results indicate that the key trigger

for cell death caused by T-P is methylation of O6-guanine, which appears to be achieved much more effectively by T-P as compared to TMZ.

The above conclusion was further confirmed by studying H2AX protein. Phosphorylation of H2AX, noted as γ-H2AX, is a marker for double strand breaks in DNA. MDA-MB-231 cells treated with T-P over a time course of 72 hours revealed substantially increased levels of γ-H2AX (***Fig. 5A***), and this effect of T-P was much stronger as compared to TMZ (***Fig. 5B***). As well, the mere combination of TMZ with POH was unable to mimic the strong induction of γ-H2AX caused by conjugated T-P (***Fig. 5C***), consistent with the CFA results shown in ***Fig. 1B*** and our notion that T-P represents a novel chemical entity different from the mix of TMZ plus POH.

The same concentration of T-P that was applied to MDA-MB-231 cells was also added to MGMT-positive MCF-7 cells. However, in this case, there was no increased phosphorylation of H2AX, consistent with the established model that MGMT rapidly repairs O6-methyl-guanine lesions; however, when these cells were pre-treated with O6-BG, increased levels of γ-H2AX became readily apparent (***Fig. 5D***). Combined, the above results characterize T-P as an alkylating agent with cytotoxic mechanism similar to TMZ, but with potency that is substantially greater than the original compound.

It is well known that GBM cells treated with physiological concentrations of TMZ (<100 μM) in vitro survive for several (5-7) days seemingly unaffected before substantial cell death becomes apparent (13, 36). We observed a similar phenotype when breast cancer cell lines were treated with T-P, i.e., cell cultures only began to deteriorate approximately a week after the onset of drug treatment. In order to characterize T-P-induced cell death in greater detail, we treated MDA-MB-231 cells with 15 μM of the drug and collected cell lysates daily over the course of 6 days. The lysates were analyzed by Western blot for the presence of two apoptosis markers, cleaved (i.e. activated) caspase 7 and cleaved PARP-1 (poly ADP-ribose polymerase-

1), along with the DNA damage marker γ-H2AX. As above, T-P treatment resulted in pronounced increase in γ-H2AX expression levels, which—except for an unexplained dip at 3 days—continued to increase over time (***Fig. 6A***). Both active caspase 7 and cleaved PARP started to increase at day 3 and remained elevated for several more days until day 6 (***Fig. 6A***), which is about the time when microscopic examination of treated cells reveals increasing deterioration of the monolayer. These results indicate that T-P-induced cell death, similar to what has been reported for physiological concentrations of TMZ, is a slow process and involves apoptotic mechanisms.

As we had shown in ***Fig. 1B***, an equimolar combination of TMZ + POH was unable to achieve the same potency in blocking colony survival as the T-P conjugate. Having established T-P's impact on DNA damage and its activation of apoptosis, we next determined whether T-P's superior effect would also be reflected at the molecular level of these marker proteins. We therefore treated cells with the same concentration (20 μM) of T-P, TMZ, POH, or TMZ combined with POH (TMZ+POH), and analyzed the induction of γ-H2AX, activated caspase 7, and cleaved PARP. As shown in ***Fig. 6B***, all three indicator proteins were induced quite prominently by T-P after 5 days of treatment, whereas TMZ or TMZ+POH exerted noticeably weaker effects and POH alone was inactive in these measurements. Thus, the results from the cell survival assay (***Fig. 1A***) correlated closely with the effects of these compounds on DNA damage and apoptosis markers (***Fig. 6B***), and in all cases T-P clearly generated the strongest anticancer impact.

Next, we wanted to address the question why T-P was more potent than TMZ. TMZ is a prodrug, and it is well known that its activation takes place spontaneously in aqueous solution at 37˚C (i.e., no cellular functions are required for this conversion). As well, the half-lives of both prodrug and active product are fairly short, where all cytotoxic triggers are set within the first few hours of treatment. To evaluate whether T-P and TMZ differed in their half-lives, we determined

how quickly, and for how long, the drugs unfolded their cytotoxic activity in cell culture. First, we exposed cells to variably short periods of drug treatment, washed off the drug, and then continued to keep cells in medium without drug to determine survival and colony-forming ability. For most of these experiments, we used 15 μM T-P and 30 μM TMZ, because these concentrations are approximately equipotent in the >90% cytotoxicity range (when measured by CFAs and a drug exposure time of 24 hours).

As shown in ***Fig. 7A*** (right two bars), exposure of cells to 15 μM T-P or 30 μM TMZ resulted in about 3% and 8% colony survival, respectively, when drugs remained in the medium for 24 hours. Yet, despite T-P unfolding slightly more potency over the course of 24 hours, TMZ displayed noticeably greater efficacy when cells were exposed for shorter time periods. As shown in ***Fig. 7A***, a one-hour exposure to TMZ reduced colony formation by >50%, whereas during the same time period T-P reduced it by only 20%; similarly, a two-hour exposure to TMZ had more than double the cytotoxic impact (23% survival) than T-P (51%). Thus, TMZ acted more quickly than T-P; it required only 4 hours to exert maximum toxicity, whereas T-P had not yet reached its maximum impact at this time point.

We next modified this experiment as follows. After cells had been exposed to drug treatment for the specific times shown in ***Fig. 7A***, we removed the medium containing the drug from the cells, and transferred this supernatant to fresh cells, which were then exposed for 24 hours. In essence, we intended to determine how much cytotoxic activity remained in each supernatant. As shown in ***Fig. 7B*** (right two bars), when supernatant was transferred after prior 24-hours of incubation, no cytotoxic activity remained, i.e., there was no reduction in colony-forming ability of the receiving cells. In contrast, when supernatant was transferred after prior one-hour incubation, colony-forming ability of receiving cells was 48% in cells receiving TMZ-containing supernatant, and 22% in T-P-containing supernatant. Even more strikingly, TMZ-containing supernatant had lost all of its activity when transferred after 4 hours, whereas T-P-

containing supernatant still contained nearly 50% of its cytotoxic activity (***Fig. 7B***). Together, these results demonstrate that T-P retained its cytotoxic potency substantially longer than TMZ.

To exclude the involvement of cellular enzymes in the turnover of T-P, we incubated T-P (and TMZ) in phosphate-buffered saline at 37˚C for one hour (in the absence of cells). After this pre-incubation, T-P and TMZ were added to cells for 24 hours, and survival was determined by CFA. As a control, both drugs were also added to cells without prior incubation in aqueous solution. A representative CFA is shown in ***Fig. 7C***, where the middle panel confirms that both drugs were used at approximately equipotent concentrations; i.e., when added straight to cells, they reduced survival by ~95%. However, pre-incubation in aqueous solution for only one hour preempted the cytotoxic potency of TMZ by about 50%, but that of T-P much less (80% remaining; see right panel). Altogether, these results establish that T-P is more stable than TMZ, suggesting that its increased potency over TMZ might be due to longer half-life, which may provide for extended opportunity to inflict cytotoxic DNA damage.

Lastly, we asked whether T-P would be able to exert its anticancer effects in vivo as well and whether it would be able to do so with a mouse tumor model representing breast cancer spread to the brain. We used D3H2LN cells, which are a bioluminescent variant of the MDA-MB-231 cell line with aggressive tumor growth in mice (31). These cells were implanted into the brains of nude mice, and 10 days later all animals were imaged for luciferase expression in order to confirm efficient tumor take.

Animals were distributed into three groups and treated once daily for 10 days with vehicle alone (control), 25 mg/kg T-P, or 25 mg/kg TMZ. This T-P dosage was chosen because our initial histopathological analysis showed that it was well tolerated by the animals (see details in ***Suppl. Fig. S3***). As summarized in ***Fig. 8A***, animals were imaged again after the termination of treatment. All vehicle-only treated animals exhibited much increased bioluminescent radiance (indicative of vigorous intracranial tumor growth (37)), some of which had conspicuously spread along the spine. Most of these animals also exhibited behavioral signs of neurological problems,

which necessitated euthanasia. In stark contrast, all animals in the T-P-treated group seemed to thrive, and their imaging analysis after the treatment period showed only small changes in radiance (***Fig. 8A***), with 3 animals presenting with radiance (tumor growth) that was lower than before the onset of treatment (see details for all animals in ***Suppl. Fig. S4***). In comparison, tumor growth in the TMZ-treated group showed generally greater bioluminescence, indicating that therapeutic efficacy of TMZ was substantially weaker than that of T-P. Overall however, the TMZ-treated group fared somewhat better than the vehicle-treated group, but clearly worse than the animals treated with T-P (***Suppl. Fig. S4***). There was some weight loss in animals from all treatment groups, but the weight of T-P-treated animals increased again after the cessation of treatment (***Suppl. Fig. S5***).

All animals were cared for and observed in the absence of any further drug treatment. As summarized by Kaplan-Meier survival plot (***Fig. 8B***), vehicle-treated animals were moribund by day 20 and had to be euthanized within the following four days (median survival: 22 days). TMZ-treated animals survived somewhat longer (median survival: 28 days). Remarkably, by day 36, when all TMZ-treated animals had succumbed to disease, all T-P-treated animals were still alive with no obvious signs of distress. Median survival of T-P-treated animals turned out to be 50 days, i.e., they survived an additional 30 days after the termination of treatment, as compared to TMZ-treated animals, which survived only an additional 8 days after treatment. Altogether, these results demonstrate potent anticancer effects of T-P that are considerably stronger than those of TMZ in vitro and in vivo.

As shown in the in vitro experiments in ***Fig. 1B***, merely mixing TMZ with POH was unable to mimic the strong cytotoxic activity of conjugated T-P. We next investigated whether this was also true under in vivo conditions. Mice with intracranial tumor burden were treated with vehicle alone, TMZ or POH alone, and with a combination of TMZ plus POH for 10 days. As shown in ***Suppl. Fig. S6***, there was no statistically significant difference (p=0.41) in survival of animals treated with TMZ alone vs. a combination of TMZ with POH, emphasizing that a mix of

TMZ plus POH is unable to enhance cytotoxic outcomes over TMZ alone. Combined with the results shown in ***Fig. 1B*** and ***Fig. 8***, it shows that the strong potency of the conjugated T-P compound in vitro and in vivo cannot be achieved by merely mixing its individual components.

4. Discussion

A landmark phase III trial completed 10 years ago (38) established a significant survival benefit for the alkylating agent temozolomide when added to radiotherapy (plus surgery when possible) for newly diagnosed glioblastoma. TMZ prolonged median survival from 12.1 to 14.6 months (38), and increased 5-year overall survival 5-fold from 1.9 to 9.8% (39). Altogether, these positive outcomes have cemented TMZ plus radiotherapy as the current standard of care for most patients with GBM. As would be expected, this approach was also evaluated for activity against intracranial metastases secondary to primary tumors of the lung, breast, and other extracranial sites. However, the results of several phase II trials (4-8) in heavily pretreated patients were not impressive enough to establish this regimen as a standard of care for instances of metastatic spread to the brain from cancers such as breast carcinoma. We therefore sought to create a novel analog of TMZ with superior activity against brain metastases.

TMZ acts as a prodrug. Its mechanism of activation involves hydrolytic opening of its tetrazinone ring, which takes places spontaneously in aqueous solution at 37˚C, and does not require the participation of cellular enzymes. The resulting product, the unstable monomethyl MTIC (5-(3-methyltriazen-1-yl)-imidazole-4-carboxamide), reacts with water to liberate AIC (4-amino-5-imidazole-carboxamide) and the highly reactive methyldiazonium cation, which methylates DNA purine residues (40, 41). Inspired by earlier studies that have demonstrated activity of perillyl alcohol in patients with GBM (25, 26), we created a novel TMZ analog where POH was covalently conjugated to the C-8 position of TMZ, resulting in T-P. In the past, extensive molecular modeling studies of antitumor imidazotetrazines (e.g., (42-44)), including

TMZ, showed that the initial activating ring-opening reaction, involving nucleophilic addition at C-4 of the tetrazinone ring, is not affected by bulky moieties at C-8. Therefore, irrespective of the nature of the targeting group conjugated at C-8, the final step in the activation process would be expected to release the electrophilic methyldiazonium ion that methylates nucleophilic sites in DNA. Based on these earlier structural and bioactivity studies, we predicted that T-P would preserve the release of the reactive methyldiazonium, and therefore that the cytotoxic activity of T-P would involve DNA methylation, similar to its parental molecule TMZ.

Our data are indeed consistent with the above mechanistic model. For instance, we show that the presence of MGMT, which highly specifically repairs O6-methylguanine and provides profound protection against TMZ (10, 11), minimizes DNA damage caused by T-P (***Fig. 5D***) and increases cellular resistance to this agent (***Fig. 3B***). Conversely, the presence of O6-BG, a specific inhibitor of MGMT, substantially enhances DNA damage caused by T-P (***Fig. 5D***) and increases this agent's cytotoxic potency exclusively in MGMT-positive cells (***Fig. 4***). As well, T-P treatment of cells leads to a reduction in MGMT protein levels (***Fig. 2C***), which is a well-established effect in the case of TMZ, due to the DNA repair enzyme's "suicide" mechanism of action, whereby acceptance of the alkyl group from O6-methylguanine leads to the protein's rapid degradation (45).

While our data establish DNA alkylation by T-P as a key mechanism by which this agent exerts its cytotoxic effect, we cannot exclude the possibility that its POH moiety may contribute additional functions. POH is known to affect several intracellular processes. For instance, it has been shown to inhibit the activity of telomerase and of sodium-potassium pump (Na+/K+-ATPase) (46, 47). As well, it has been described as a farnesyl-transferase inhibitor that results in the blockage of ras oncoprotein activity (48, 49), although this has been challenged (50, 51). Importantly, in all these cases relatively high concentrations of POH (well above 100 μM) are required to achieve 50% inhibition of target activity (see also ***Fig. 1B***). In comparison, T-P is active in the range of 1-5 μM in MGMT-negative cells (***Table 1***). Notably as well, when POH is

mixed with TMZ and applied as a separate agent, this combination is unable to replicate the high potency of conjugated T-P (***Figs. 1B, 5C, 6B***), indicating that the mere presence of non-conjugated POH is unable to provide additional potency over TMZ. These considerations, combined with T-P's notable sensitivity to MGMT and O6-BG as detailed above, diminish the likelihood for involvement of functions other than DNA damage.

If conjugation of POH indeed does not provide additional pro-apoptotic mechanisms over TMZ alone, why is T-P significantly more potent than TMZ? It has been well established that TMZ (and its active degradation product) exhibits rapid turnover in vitro and in vivo, with a half-life in the range of 1-2 hours (32, 43). Consistent with these characteristics, we find that after 4 hours of incubation in medium, nearly 100% of TMZ's cytotoxic activity has been spent (***Fig. 7***). In contrast, T-P appears significantly longer-lived, where after 4 hours about 50% activity remains (***Fig. 7***). We therefore propose that the extended presence of T-P may provide for greater opportunity to set DNA lesions, resulting in increased cytotoxicity.

While the extended half-life of T-P may suffice to explain its greater potency in vitro, it remains to be established whether it also contributes to its substantially increased in vivo potency in our brain metastasis model (***Fig. 8***). Because the lipophilicity of T-P is increased over TMZ (data not shown), it is also possible that T-P may cross the BBB more efficiently than TMZ. In the case of TMZ, it is known that drug levels achieved in the cerebrospinal fluid (CSF) are 80% lower than drug levels in the systemic circulation, i.e., in plasma (52). It is therefore conceivable that TMZ, despite its established therapeutic benefit, would exert even greater activity, if only higher intracranial concentrations could be achieved. In this regard, T-P might be the vehicle to achieve this, and detailed physicochemical and pharmacokinetic studies are planned to investigate this aspect.

It is quite intriguing that TMZ displayed only minor activity in our intracranial in vivo model (***Fig. 8***). The breast cancer cell line we used, a variant of MDA-MB-231, does exhibit exquisite in vitro sensitivity to TMZ (IC50 <10 μM), and therefore is more sensitive to TMZ than

most MGMT-negative GBM cell lines reported in the literature (e.g. (53)) and inclusive of several GBM cell lines we analyzed in parallel (data not shown). As well, the TMZ dosage used (25 mg/kg) is well within the range of dosages shown to exert potent activity in GBM mouse models, where even 5 mg/kg has significant activity (30). We therefore speculate that the triple-negative 231 cell line might harbor intrinsic mechanisms of resistance to TMZ that emerge only in the in vivo environment, and perhaps are reflective of the unimpressive responses that were noted when breast cancer patients with brain metastases were treated with TMZ (6, 8). While this conjecture remains hypothetical at this time, it is obvious from our studies that T-P provides far superior therapeutic benefit than TMZ in our intracranial tumor model (***Fig. 8***), which may bode well for the clinical setting. We therefore propose that T-P should be investigated further as a potentially effective addition to therapeutic regimens for brain-metastatic breast cancer.

Disclosure of Potential Clonflicts of Interest

TCC is founder and stakeholder of NeOnc Technologies, Woodland Hills, CA.

Acknowledgements

We thank Drs. Michael F. Press and Steve Swenson (University of Southern California) for providing breast cancer cell lines. We are grateful to Dr. Bernd Kaina (University of Würzburg, Germany) for the gift of plasmids containing MGMT cDNA and the neo gene. We thank Drs. Daniel Levin and Satish Puppali (Norac Pharma, Azusa CA) for T-P conjugation and API manufacturing, and NeOnc Technologies (Woodland Hills, CA) for providing T-P. We acknowledge patient advocate Diana T. Chingos for providing input from the patient's perspective.

References

1. Quigley MR, Fukui O, Chew B, Bhatia S, Karlovits S. The shifting landscape of metastatic breast cancer to the CNS. Neurosurg Rev 2013;36:377-82.

2. Lockman PR, Mittapalli RK, Taskar KS, Rudraraju V, Gril B, Bohn KA, et al. Heterogeneous blood-tumor barrier permeability determines drug efficacy in experimental brain metastases of breast cancer. Clin Cancer Res 2010;16:5664-78.

3. Zhang J, Stevens MF, Bradshaw TD. Temozolomide: mechanisms of action, repair and resistance. Curr Mol Pharmacol 2012;5:102-14.

4. Christodoulou C, Bafaloukos D, Kosmidis P, Samantas E, Bamias A, Papakostas P, et al. Phase II study of temozolomide in heavily pretreated cancer patients with brain metastases. Annals Oncol 2001;12:249-54.

5. Abrey LE, Olson JD, Raizer JJ, Mack M, Rodavitch A, Boutros DY, et al. A phase II trial of temozolomide for patients with recurrent or progressive brain metastases. J Neurooncol 2001;53:259-65.

6. Trudeau ME, Crump M, Charpentier D, Yelle L, Bordeleau L, Matthews S, et al. Temozolomide in metastatic breast cancer (MBC): a phase II trial of the National Cancer Institute of Canada - Clinical Trials Group (NCIC-CTG). Annals Oncol 2006;17:952-6.

7. Addeo R, De Rosa C, Faiola V, Leo L, Cennamo G, Montella L, et al. Phase 2 trial of temozolomide using protracted low-dose and whole-brain radiotherapy for nonsmall cell lung cancer and breast cancer patients with brain metastases. Cancer 2008;113:2524-31.

8. Siena S, Crino L, Danova M, Del Prete S, Cascinu S, Salvagni S, et al. Dose-dense temozolomide regimen for the treatment of brain metastases from melanoma, breast cancer, or lung cancer not amenable to surgery or radiosurgery: a multicenter phase II study. Annals Oncol 2010;21:655-61.

9. Addeo R, Sperlongano P, Montella L, Vincenzi B, Carraturo M, Iodice P, et al. Protracted low dose of oral vinorelbine and temozolomide with whole-brain radiotherapy in the treatment for breast cancer patients with brain metastases. Cancer Chemother Pharmacol 2012;70:603-9.

10. Pegg AE. Multifaceted roles of alkyltransferase and related proteins in DNA repair, DNA damage, resistance to chemotherapy, and research tools. Chem Res Toxicol 2011;24:618-39.

11. Christmann M, Verbeek B, Roos WP, Kaina B. O(6)-Methylguanine-DNA methyltransferase (MGMT) in normal tissues and tumors: enzyme activity, promoter methylation and immunohistochemistry. Biochim Biophys Acta 2011;1816:179-90.

12. Silber JR, Bobola MS, Blank A, Chamberlain MC. O(6)-methylguanine-DNA methyltransferase in glioma therapy: promise and problems. Biochim Biophys Acta 2012;1826:71-82.

13. Knizhnik AV, Roos WP, Nikolova T, Quiros S, Tomaszowski KH, Christmann M, et al. Survival and death strategies in glioma cells: autophagy, senescence and apoptosis triggered by a single type of temozolomide-induced DNA damage. PLoS One 2013;8:e55665.

14. Ingold B, Schraml P, Heppner FL, Moch H. Homogeneous MGMT immunoreactivity correlates with an unmethylated MGMT promoter status in brain metastases of various solid tumors. PLoS One 2009;4:e4775.

15. Kaina B, Margison GP, Christmann M. Targeting O(6)-methylguanine-DNA methyltransferase with specific inhibitors as a strategy in cancer therapy. Cell Mol Life Sci 2010;67:3663-81.

16. Pegg AE, Wiest L, Mummert C, Stine L, Moschel RC, Dolan ME. Use of antibodies to human O6-alkylguanine-DNA alkyltransferase to study the content of this protein in cells treated with O6-benzylguanine or N-methyl-N'-nitro-N-nitrosoguanidine. Carcinogenesis 1991;12:1679-83.

17. Kaina B, Christmann M, Naumann S, Roos WP. MGMT: key node in the battle against genotoxicity, carcinogenicity and apoptosis induced by alkylating agents. DNA Repair (Amst) 2007;6:1079-99.

18. Quinn JA, Jiang SX, Reardon DA, Desjardins A, Vredenburgh JJ, Rich JN, et al. Phase II trial of temozolomide plus o6-benzylguanine in adults with recurrent, temozolomide-resistant malignant glioma. J Clin Oncol 2009;27:1262-7.

19. Belanger JT. Perillyl alcohol: applications in oncology. Altern Med Rev 1998;3:448-57.

20. Haag JD, Gould MN. Mammary carcinoma regression induced by perillyl alcohol, a hydroxylated analog of limonene. Cancer Chemother Pharmacol 1994;34:477-83.

21. Mills JJ, Chari RS, Boyer IJ, Gould MN, Jirtle RL. Induction of apoptosis in liver tumors by the monoterpene perillyl alcohol. Cancer Res 1995;55:979-83.

22. Liu G, Oettel K, Bailey H, Ummersen LV, Tutsch K, Staab MJ, et al. Phase II trial of perillyl alcohol (NSC 641066) administered daily in patients with metastatic androgen independent prostate cancer. Invest New Drugs 2003;21:367-72.

23. Bailey HH, Attia S, Love RR, Fass T, Chappell R, Tutsch K, et al. Phase II trial of daily oral perillyl alcohol (NSC 641066) in treatment-refractory metastatic breast cancer. Cancer Chemother Pharmacol 2008;62:149-57.

24. Meadows SM, Mulkerin D, Berlin J, Bailey H, Kolesar J, Warren D, et al. Phase II trial of perillyl alcohol in patients with metastatic colorectal cancer. Int J Gastrointest Cancer 2002;32:125-8.

25. da Fonseca CO, Simao M, Lins IR, Caetano RO, Futuro D, Quirico-Santos T. Efficacy of monoterpene perillyl alcohol upon survival rate of patients with recurrent glioblastoma. J Cancer Res Clin Oncol 2011;137:287-93.

26. da Fonseca CO, Schwartsmann G, Fischer J, Nagel J, Futuro D, Quirico-Santos T, et al. Preliminary results from a phase I/II study of perillyl alcohol intranasal administration in adults with recurrent malignant gliomas. Surg Neurol 2008;70:259-66.

27. Yoneda T, Williams PJ, Hiraga T, Niewolna M, Nishimura R. A bone-seeking clone exhibits different biological properties from the MDA-MB-231 parental human breast cancer cells and a brain-seeking clone in vivo and in vitro. J Bone Miner Res 2001;16:1486-95.

28. Kaina B, Fritz G, Mitra S, Coquerelle T. Transfection and expression of human O6-methylguanine-DNA methyltransferase (MGMT) cDNA in Chinese hamster cells: the role of MGMT in protection against the genotoxic effects of alkylating agents. Carcinogenesis 1991;12:1857-67.

29. Pyrko P, Soriano N, Kardosh A, Liu YT, Uddin J, Petasis NA, et al. Downregulation of survivin expression and concomitant induction of apoptosis by celecoxib and its non-cyclooxygenase-2-inhibitory analog, dimethyl-celecoxib (DMC), in tumor cells in vitro and in vivo. Mol Cancer 2006;5:19.

30. Chen TC, Wang W, Golden EB, Thomas S, Sivakumar W, Hofman FM, et al. Green tea epigallocatechin gallate enhances therapeutic efficacy of temozolomide in orthotopic mouse glioblastoma models. Cancer Lett 2011;302:100-8.

31. Jenkins DE, Hornig YS, Oei Y, Dusich J, Purchio T. Bioluminescent human breast cancer cell lines that permit rapid and sensitive in vivo detection of mammary tumors and multiple metastases in immune deficient mice. Breast Cancer Res 2005;7:R444-54.

32. Brada M, Judson I, Beale P, Moore S, Reidenberg P, Statkevich P, et al. Phase I dose-escalation and pharmacokinetic study of temozolomide (SCH 52365) for refractory or relapsing malignancies. Br J Cancer 1999;81:1022-30.

33. Marzolini C, Decosterd LA, Shen F, Gander M, Leyvraz S, Bauer J, et al. Pharmacokinetics of temozolomide in association with fotemustine in malignant melanoma and malignant glioma patients: comparison of oral, intravenous, and hepatic intra-arterial administration. Cancer Chemother Pharmacol 1998;42:433-40.

34. Cho HY, Wang W, Jhaveri N, Torres S, Tseng J, Leong MN, et al. Perillyl alcohol for the treatment of temozolomide-resistant gliomas. Mol Cancer Ther 2012;11:2462-72.

35. Yuri T, Danbara N, Tsujita-Kyutoku M, Kiyozuka Y, Senzaki H, Shikata N, et al. Perillyl alcohol inhibits human breast cancer cell growth in vitro and in vivo. Breast Cancer Res 2004;84:251-60.

36. Hirose Y, Berger MS, Pieper RO. p53 effects both the duration of G2/M arrest and the fate of temozolomide-treated human glioblastoma cells. Cancer Res 2001;61:1957-63.

37. Szentirmai O, Baker CH, Lin N, Szucs S, Takahashi M, Kiryu S, et al. Noninvasive bioluminescence imaging of luciferase expressing intracranial U87 xenografts: correlation with magnetic resonance imaging determined tumor volume and longitudinal use in assessing tumor growth and antiangiogenic treatment effect. Neurosurgery 2006;58:365-72.

38. Stupp R, Mason WP, van den Bent MJ, Weller M, Fisher B, Taphoorn MJ, et al. Radiotherapy plus concomitant and adjuvant temozolomide for glioblastoma. N Engl J Med 2005;352:987-96.

39. Stupp R, Hegi ME, Mason WP, van den Bent MJ, Taphoorn MJ, Janzer RC, et al. Effects of radiotherapy with concomitant and adjuvant temozolomide versus radiotherapy alone on survival in glioblastoma in a randomised phase III study: 5-year analysis of the EORTC-NCIC trial. Lancet Oncol 2009;10:459-66.

40. Denny BJ, Wheelhouse RT, Stevens MF, Tsang LL, Slack JA. NMR and molecular modeling investigation of the mechanism of activation of the antitumor drug temozolomide and its interaction with DNA. Biochemistry 1994;33:9045-51.

41. Saleem A, Brown GD, Brady F, Aboagye EO, Osman S, Luthra SK, et al. Metabolic activation of temozolomide measured in vivo using positron emission tomography. Cancer Res 2003;63:2409-15.

42. Arrowsmith J, Jennings SA, Clark AS, Stevens MF. Antitumor imidazotetrazines. 41. Conjugation of the antitumor agents mitozolomide and temozolomide to peptides and lexitropsins bearing DNA major and minor groove-binding structural motifs. J Med Chem 2002;45:5458-70.

43. Clark AS, Deans B, Stevens MF, Tisdale MJ, Wheelhouse RT, Denny BJ, et al. Antitumor imidazotetrazines. 32. Synthesis of novel imidazotetrazinones and related bicyclic

heterocycles to probe the mode of action of the antitumor drug temozolomide. J Med Chem 1995;38:1493-504.

44. Lunt E, Newton CG, Smith C, Stevens GP, Stevens MF, Straw CG, et al. Antitumor imidazotetrazines. 14. Synthesis and antitumor activity of 6- and 8-substituted imidazo[5,1-d]-1,2,3,5-tetrazinones and 8-substituted pyrazolo[5,1-d]-1,2,3,5-tetrazinones. J Med Chem 1987;30:357-66.

45. Xu-Welliver M, Pegg AE. Degradation of the alkylated form of the DNA repair protein, O(6)-alkylguanine-DNA alkyltransferase. Carcinogenesis 2002;23:823-30.

46. Garcia DG, Amorim LM, de Castro Faria MV, Freire AS, Santelli RE, Da Fonseca CO, et al. The anticancer drug perillyl alcohol is a Na/K-ATPase inhibitor. Mol Cell Biochem 2010;345:29-34.

47. Sundin T, Peffley DM, Gauthier D, Hentosh P. The isoprenoid perillyl alcohol inhibits telomerase activity in prostate cancer cells. Biochimie 2012;94:2639-48.

48. Hardcastle IR, Rowlands MG, Barber AM, Grimshaw RM, Mohan MK, Nutley BP, et al. Inhibition of protein prenylation by metabolites of limonene. Biochem Pharmacol 1999;57:801-9.

49. Crowell PL, Chang RR, Ren ZB, Elson CE, Gould MN. Selective inhibition of isoprenylation of 21-26-kDa proteins by the anticarcinogen d-limonene and its metabolites. J Biol Chem 1991;266:17679-85.

50. Karlson J, Borg-Karlson AK, Unelius R, Shoshan MC, Wilking N, Ringborg U, et al. Inhibition of tumor cell growth by monoterpenes in vitro: evidence of a Ras-independent mechanism of action. Anticancer Drugs 1996;7:422-9.

51. Ruch RJ, Sigler K. Growth inhibition of rat liver epithelial tumor cells by monoterpenes does not involve Ras plasma membrane association. Carcinogenesis 1994;15:787-9.

52. Ostermann S, Csajka C, Buclin T, Leyvraz S, Lejeune F, Decosterd LA, et al. Plasma and cerebrospinal fluid population pharmacokinetics of temozolomide in malignant glioma patients. Clin Cancer Res 2004;10:3728-36.

53. Agnihotri S, Gajadhar AS, Ternamian C, Gorlia T, Diefes KL, Mischel PS, et al. Alkylpurine-DNA-N-glycosylase confers resistance to temozolomide in xenograft models of glioblastoma multiforme and is associated with poor survival in patients. J Clin Invest 2012;122:253-66.

Author Manuscript Published OnlineFirst on March 12, 2014; DOI: 10.1158/1535-7163.MCT-13-0882
Author manuscripts have been peer reviewed and accepted for publication but have not yet been edited.

Table 1. Drug sensitivities of various breast cancer cell lines.

Cell Line	MGMT status	IC50 TMZ (μM)	IC50 T-P (μM)	Differential (-fold)
MDA-MB-231-br	—	3.8	1.2	3.2
MDA-MB-231	—	9.9	2.3	4.3
T47D	—	20	4.6	4.3
HCC-1937	+	186	31	6.0
MDA-MB-468	+	195	31	6.3
MCF7	+	513	33	15.5

Shown are IC50 values (i.e., drug concentrations that reduce colony forming ability by 50%) and differential toxicity between T-P and TMZ (i.e., fold increased potency of T-P over TMZ).

Figure Legends

Figure 1. Survival of breast cancer cells after drug treatment.

(A) Various breast cancer cell lines were exposed to increasing concentrations of TMZ (diamonds) or T-P (circles) for 48 hours, and survival was determined via colony formation assay (CFA). (B) Cells were exposed for 48 hours to increasing concentrations of TMZ (diamonds), T-P (circles), POH (triangles), or equimolar concentrations of TMZ plus POH (squares). In all graphs, colony formation by control cells (treated with vehicle only) is set at 1. Graphs with error bars display mean (±SD) from ≥3 independent experiments; graphs without error bars show the average from two independent experiments.

Figure 2. MGMT expression levels in various cell lines.

All parts show Western blot analysis of MGMT protein levels with actin as the loading control. (A) MGMT basal levels in the six breast cancer cell lines used in this study. (B) MGMT basal levels in three GBM cell lines compared to MCF7 breast cancer cells. (C) MDA-MB-468 cells were treated with the indicated concentrations of T-P, TMZ, or O6-BG for 17 hours before harvest of cellular lysates. vh.= cells treated with vehicle only.

Figure 3. Drug sensitivity of MGMT-transfected cells.

MDA-MB-231 cells were stably transfected with MGMT cDNA. (A) Two individually selected clones, 231-MGMT-1 and -2, were analyzed by Western blot for basal level MGMT protein expression in comparison to parental cells. (B) 231-MGMT-1 and -2 were treated with increasing concentrations of T-P and TMZ for 48 hours, and cell survival was analyzed by CFA. Graph with 231-MGMT-1 cells displays mean (±SD) from 3 independent experiments; graph with 231-MGMT-2 cells shows the average from two independent experiments.

Figure 4. Effect of inclusion of O6-BG.

Cells were exposed to TMZ or T-P for 48 hours with or without pretreatment with O6-BG, and cell survival was determined by CFA. Colony survival of (A) MDA-MB-231 cells, (B) MGMT-transfected 231-MGMT-1 cells, and (C) MDA-MB-468 cells. Shown is mean number of colonies (±SD) from ≥3 wells treated in parallel.

Figure 5. Drug effects on DNA damage marker.

Cells were treated with different concentrations of T-P or TMZ and analyzed by Western blot analysis for expression levels of γ-H2AX, a marker for double-strand DNA damage. Actin was used as a loading control. (A) MDA-MB-231 cells were treated with 50 μM T-P for the indicated time periods. (B) MDA-MB-231 cells were treated with 50 μM T-P or 50 μM TMZ for the indicated time periods. (C) MDA-MB-231 cells were treated with T-P, TMZ, POH, or TMZ combined with POH (all at 10 μM each) for 24 hours. (Lanes from the same blot were cut and rearranged for optimized viewing.) (D) MCF7 cells were treated with or without 50 μM T-P in the presence or absence of 30 μM O6-BG for 48 hours.

Figure 6. DNA damage and cell death marker analysis.

MDA-MB-231 cells were used for Western blot analysis of expression levels for markers of DNA damage (γ-H2AX) and cell death (activated caspase 7 and cleaved PARP). (A) Cells were treated with 15 μM T-P and harvested every 24 hours up to 6 days. Control cells remained untreated, or received vehicle (vh.) only. (B) Cells were treated with 20 μM of either T-P, TMZ, or POH individually, or with 20 μM TMZ combined with 20 μM POH (TMZ+POH) and harvested after 24 hours or 5 days. Control cells remained untreated, or received vehicle (vh.) only. In the case of caspase 7, only the activated (cleaved) form is shown (cl. C-7). In the case of PARP,

the top panel shows both full-length and proteolytically cleaved forms of the protein, whereas the bottom panel only shows faster-migrating, cleaved PARP.

Figure 7. Determination of drug stability.

MDA-MB-231 cells were analyzed in colony formation assays. (A) Cells were treated with 15 μM T-P or 30 μM TMZ for 30 min or 1, 2, 4, and 24 hours. Thereafter, drug-containing medium was removed, fresh medium (without drug) was added, and cells remained undisturbed until colony staining 12 days later. (B) Cells were exposed to supernatant (i.e., the drug-containing medium removed from cells shown in A). The arrows indicate which cells received which supernatant. After 24 hours of incubation, all drug-containing medium was removed, fresh medium (without drug) was added, and cells remained undisturbed until colony staining 12 days later. (C) Shown is a representative 6-well plate with stained colonies. Left panel (untreated): control cells without drug treatment. Middle panel (0-24h): Cells received 15 μM T-P or 30 μM TMZ for 24 hours. Right panel (1-25h): T-P and TMZ were incubated in neutral buffer at 37˚C for 1 hour before addition to cells to a final concentration of 15 μM T-P and 30 μM TMZ for 24 hours.

Figure 8. Drug effects on intracranial tumor growth.

Luciferase-positive D3H2LN cells were implanted into the brains of 24 nude mice. Ten days later, tumor take was confirmed via bioluminescent imaging, and treatment was initiated with vehicle only (control group), 25 mg/kg T-P, or 25 mg/kg TMZ, once daily over the course of 10 days. (A) All surviving animals were imaged again on days 21, 28, and 43. Shown is one representative mouse from each group. Heat bar to the right shows scale of radiance. (B) Kaplan-Meier survival plot of all animals carrying intracranial tumors. Arrow labeled Rx indicates the time period of treatment. Statistical difference between groups of TMZ-treated and T-P-treated animals: $p<0.01$.

Author Manuscript Published OnlineFirst on March 12, 2014; DOI: 10.1158/1535-7163.MCT-13-0882
Author manuscripts have been peer reviewed and accepted for publication but have not yet been edited.

Figure 1

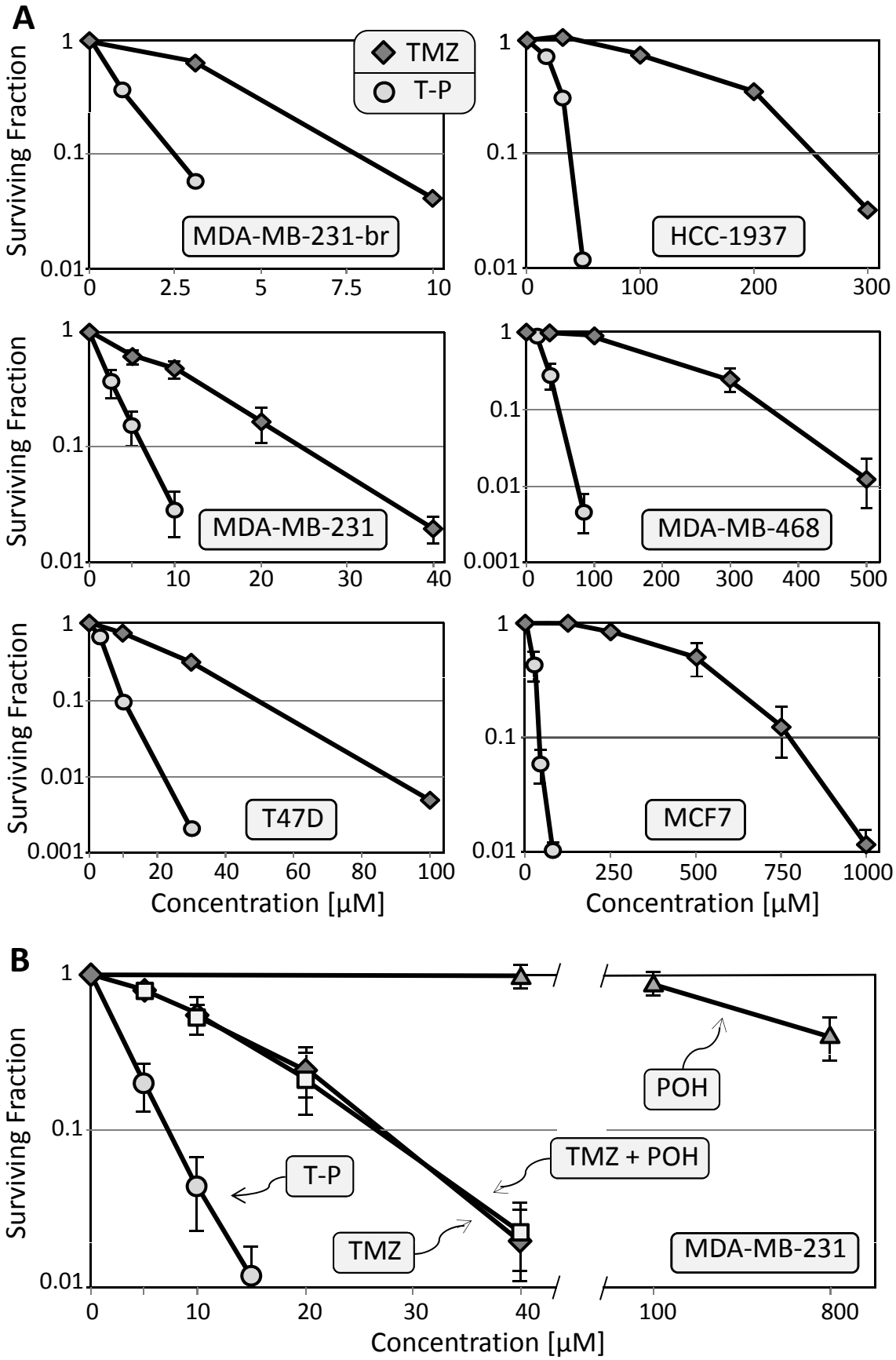

Author Manuscript Published OnlineFirst on March 12, 2014; DOI: 10.1158/1535-7163.MCT-13-0882
Author manuscripts have been peer reviewed and accepted for publication but have not yet been edited.

Figure 2

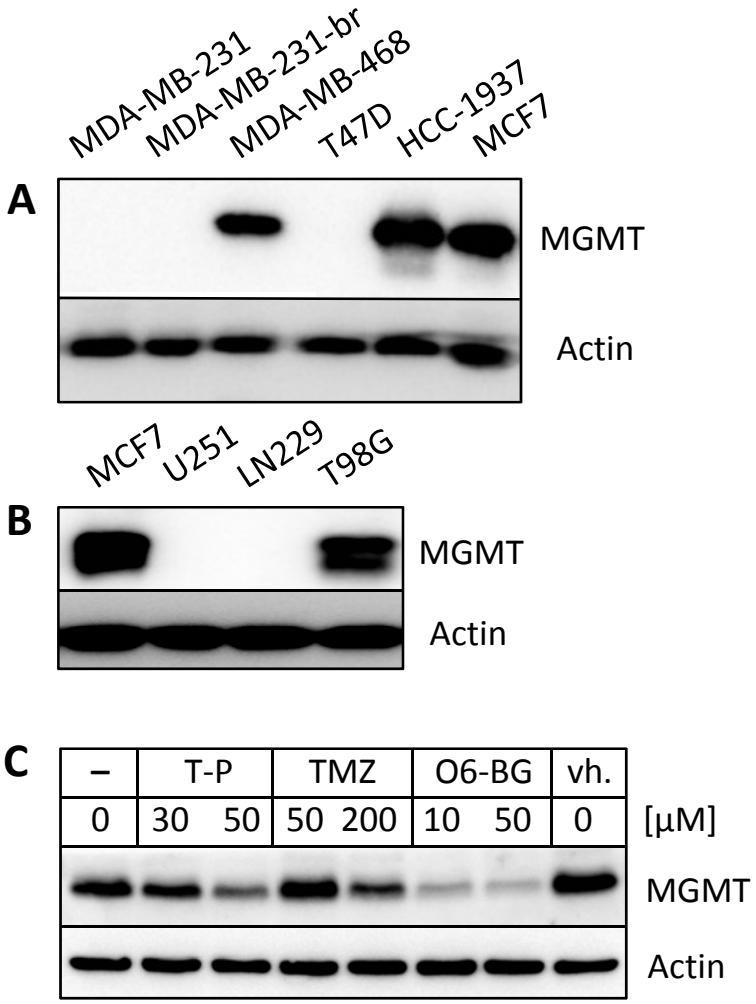

Author Manuscript Published OnlineFirst on March 12, 2014; DOI: 10.1158/1535-7163.MCT-13-0882
Author manuscripts have been peer reviewed and accepted for publication but have not yet been edited.

Figure 3

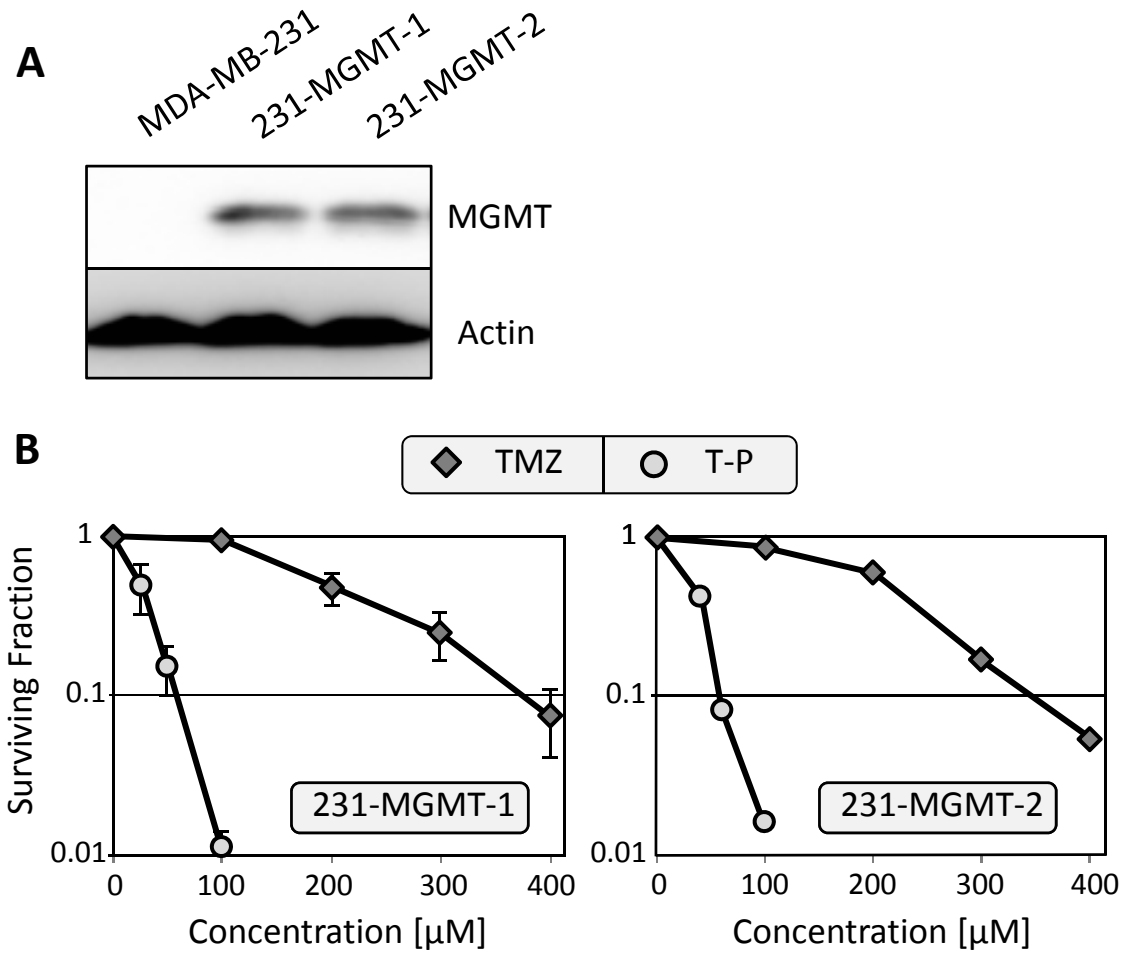

Author Manuscript Published OnlineFirst on March 12, 2014; DOI: 10.1158/1535-7163.MCT-13-0882
Author manuscripts have been peer reviewed and accepted for publication but have not yet been edited.

Figure 4

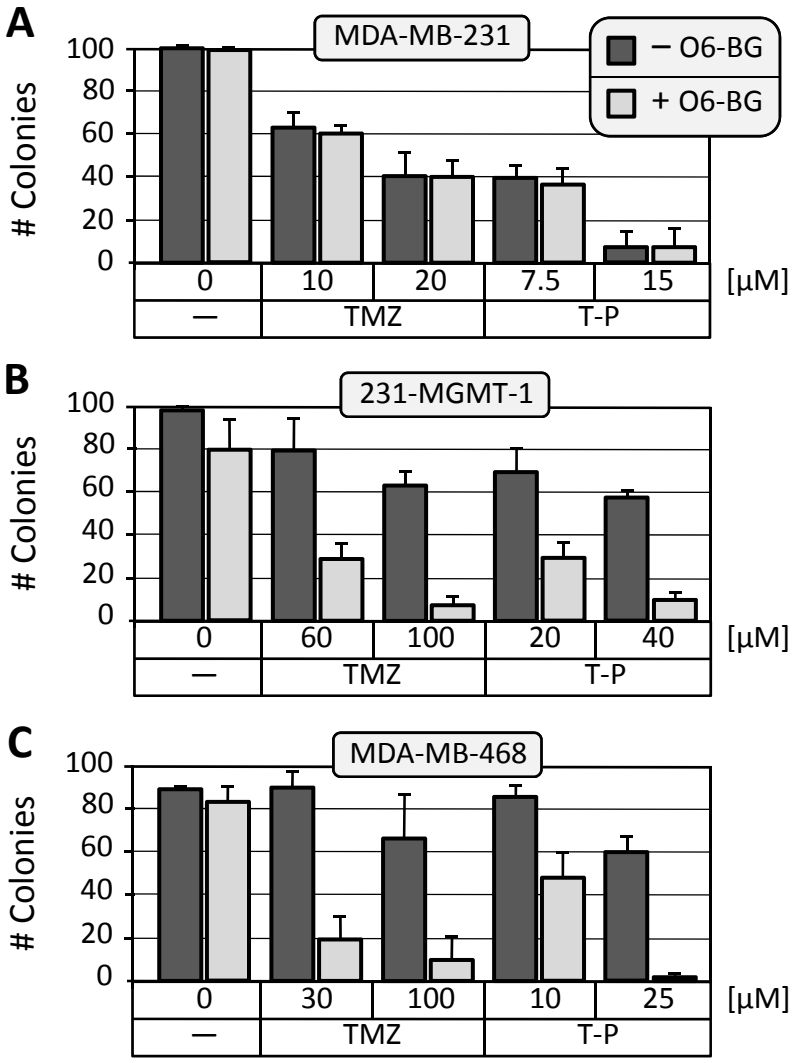

Author Manuscript Published OnlineFirst on March 12, 2014; DOI: 10.1158/1535-7163.MCT-13-0882
Author manuscripts have been peer reviewed and accepted for publication but have not yet been edited.

Figure 5

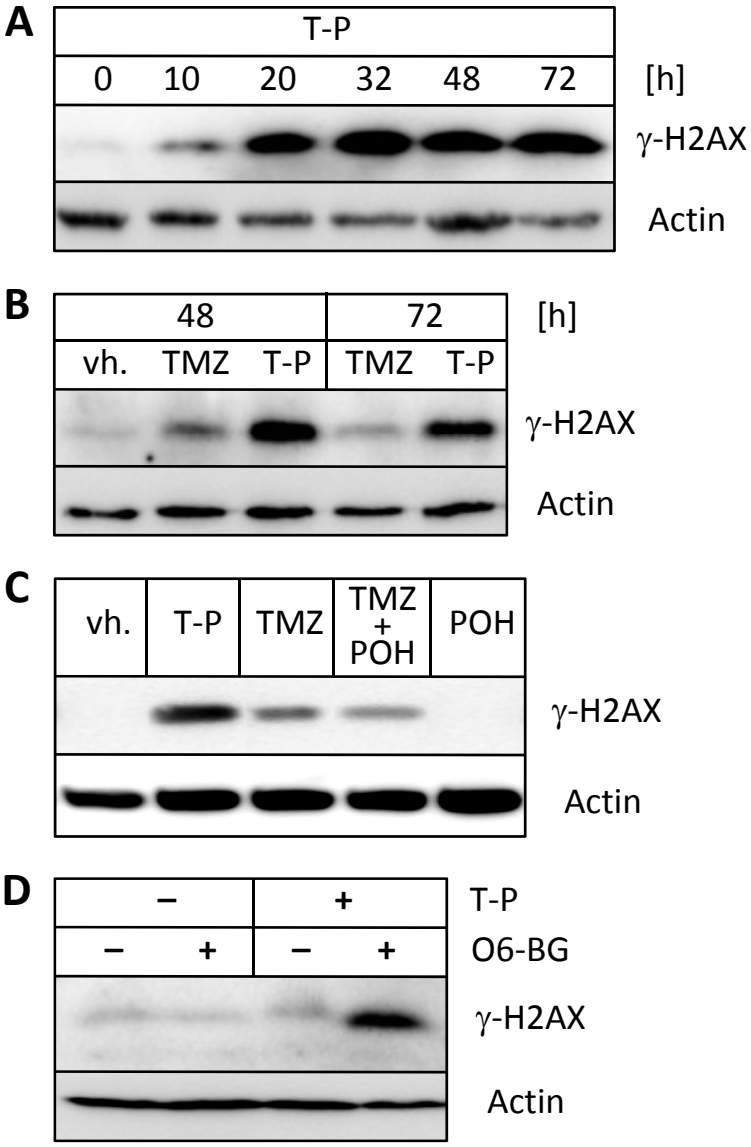

Author Manuscript Published OnlineFirst on March 12, 2014; DOI: 10.1158/1535-7163.MCT-13-0882
Author manuscripts have been peer reviewed and accepted for publication but have not yet been edited.

Figure 6

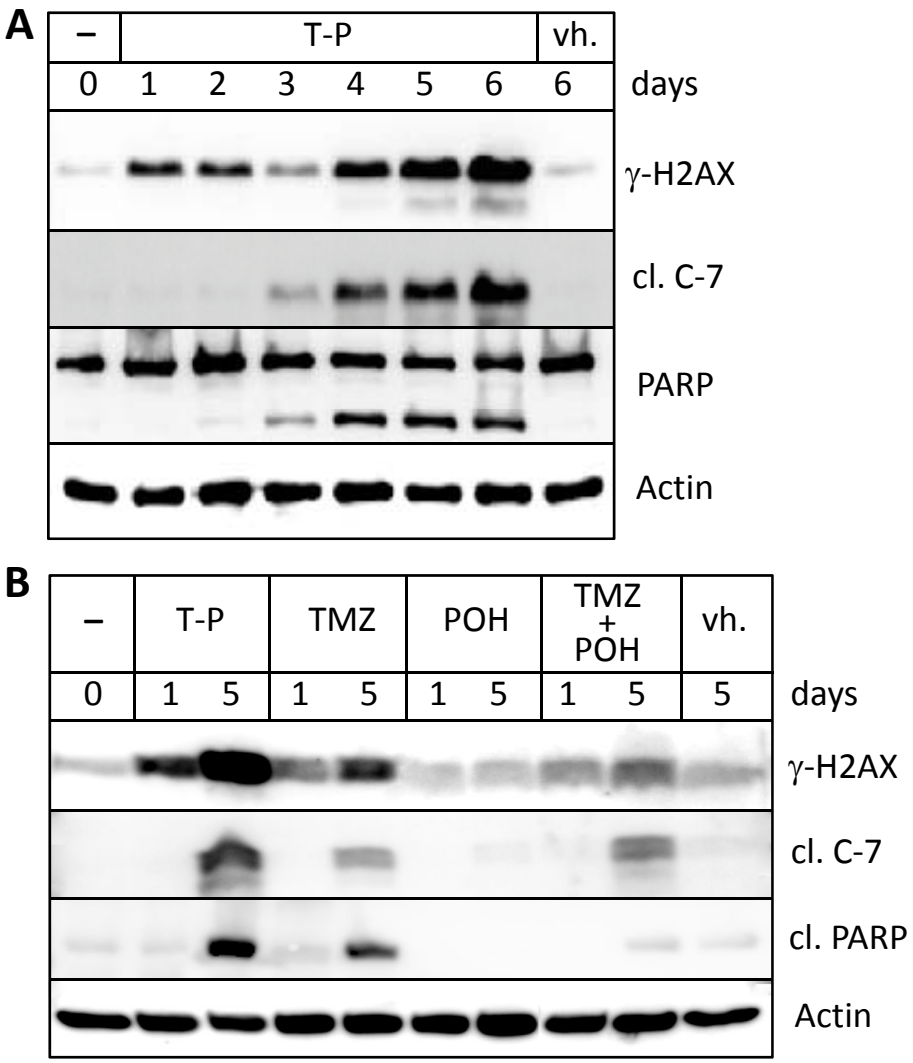

Author Manuscript Published OnlineFirst on March 12, 2014; DOI: 10.1158/1535-7163.MCT-13-0882
Author manuscripts have been peer reviewed and accepted for publication but have not yet been edited.

Figure 7

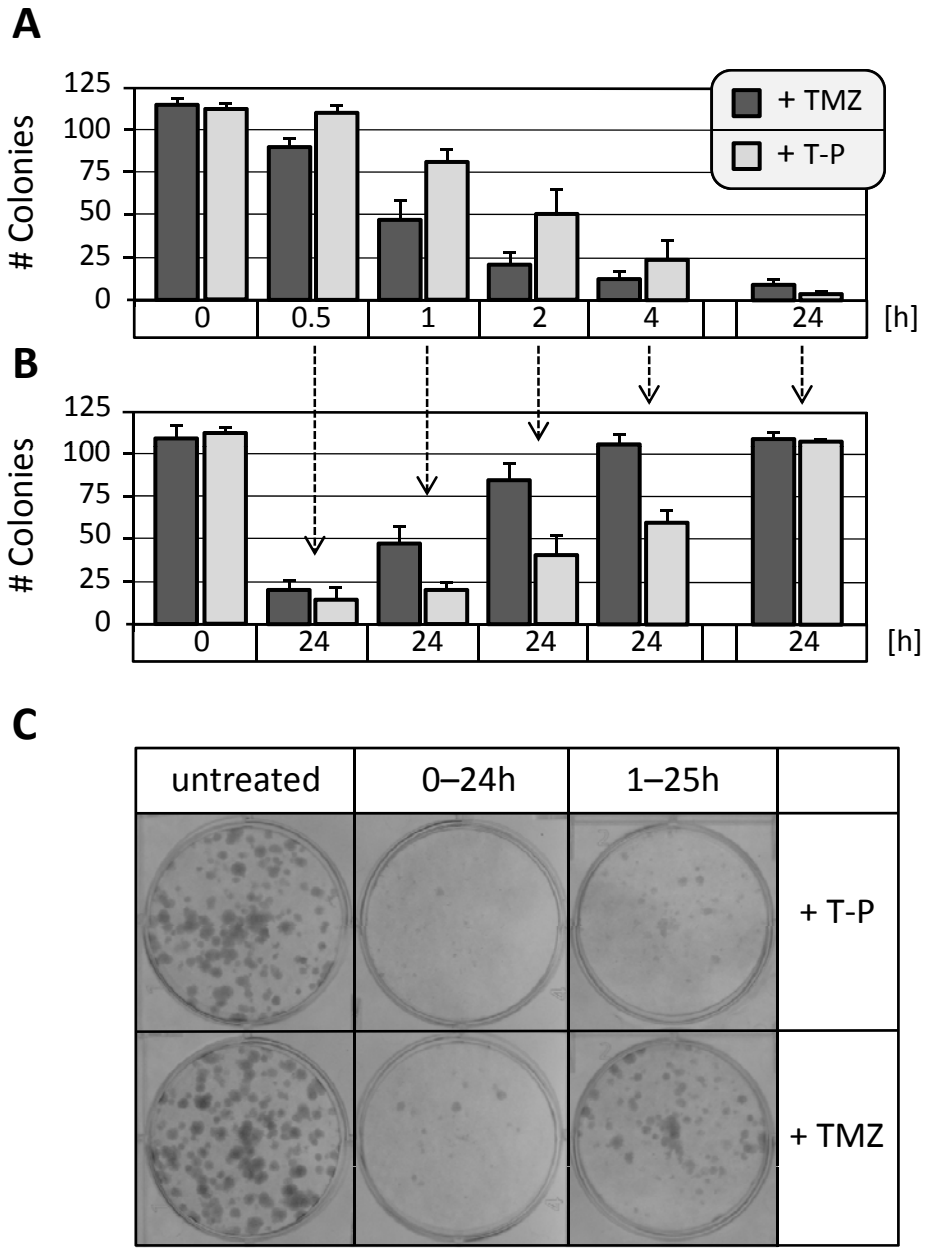

Author Manuscript Published OnlineFirst on March 12, 2014; DOI: 10.1158/1535-7163.MCT-13-0882
Author manuscripts have been peer reviewed and accepted for publication but have not yet been edited.

Figure 8

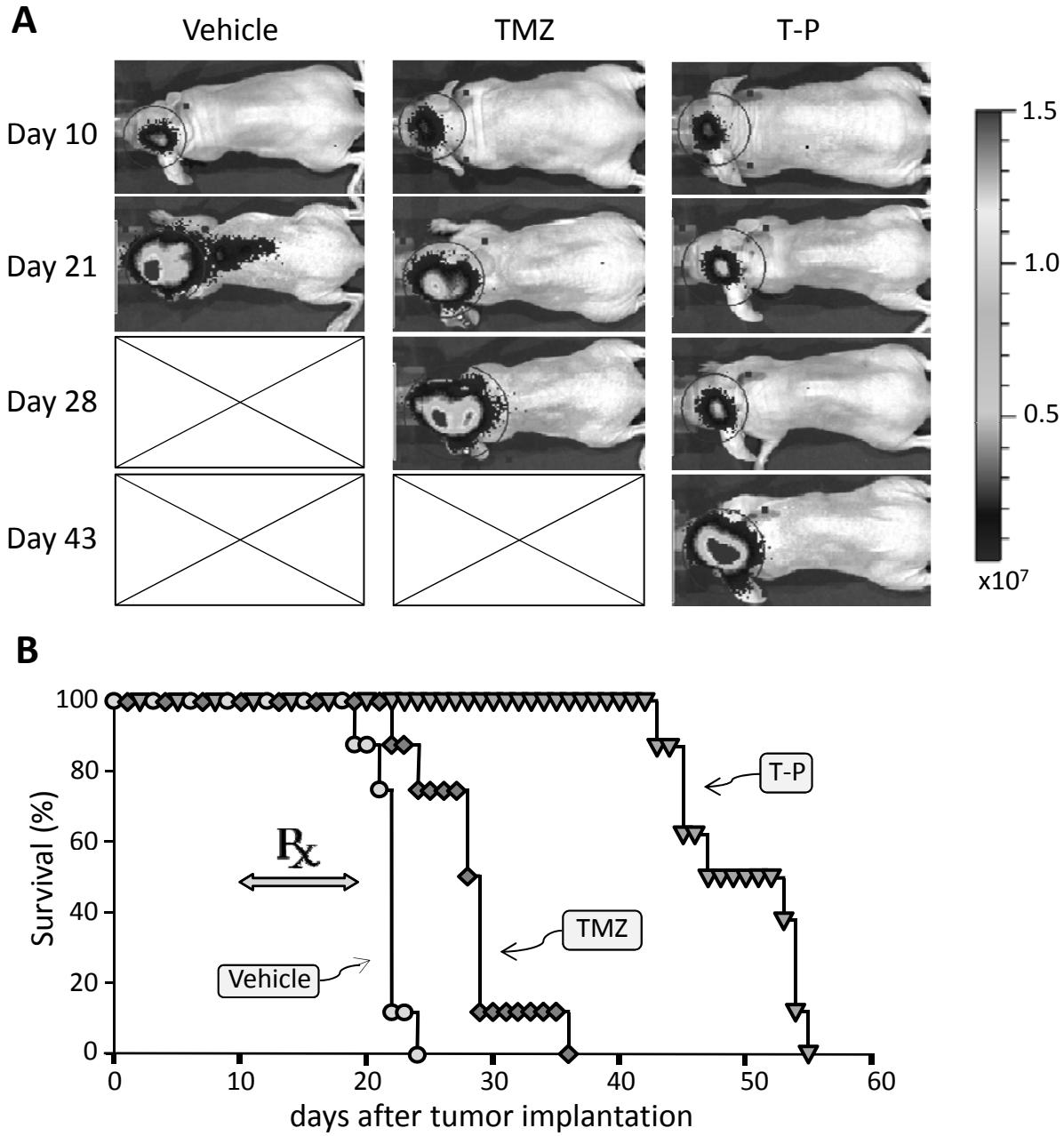

Legends to Supplementary Figures

Supplementary Figure S1. Chemical structure of T-P.

POH was covalently linked to TMZ's amide functionality via a carbonyl bridge (shown between dashed lines). The grey box indicates the TMZ moiety that forms the highly reactive methyldiazonium ion that methylates DNA after decomposition of the pro-drug TMZ in aqueous solution.

Supplementary Figure S2. Colony formation after drug treatment.

Shown is a photo of a highly representative result from a colony-formation assay in a 6-well plate. MDA-MB-231 cells were treated with 10 μM T-P or TMZ, in the presence and absence of 10 μM POH. This illustrates that 10 μM T-P blocks colony formation substantially more potently than TMZ, and that the addition of equimolar concentrations of POH to either TMZ or T-P is unable to enhance toxicity any further.

Supplementary Figure S3. Histopathological evaluation following chronic T-P treatment.

Mice received once-daily, subcutaneous injections of vehicle only, or T-P at 37 mg/kg, for 20 consecutive days. Thereafter, the animals were euthanized. Organs were collected, fixed with formalin, and stained with hematoxylin/eosin. Bone marrow smear specimens were also stained and evaluated for potential pathologic changes. (A) Representative display from vehicle-treated animals. (B) Representative display from T-P-treated animals. As shown, there were no obvious differences between vehicle-treated and T-P-treated animals, indicating that T-P did not cause obvious toxicity in normal tissues.

Supplementary Figure S4. Drug effects on intracranial tumor growth.

All tumor-bearing animals were imaged on day 10 (start of daily treatment) and day 21 (48

hours after termination of treatment). Tumor growth during the 10-day treatment period was determined indirectly via the increase in bioluminescent radiance. Shown is the fold increase in radiance for each animal between days 10 and 21 (bioluminescence on day 10 was set at 1). Four of the vehicle-treated animals were moribund or dead and could not be imaged on day 21; based on additional variables and observations (not shown), their increase in tumor growth is shown as “est.” (best estimation). One of the TMZ-treated and three of the T-P-treated animals (marked by asterisks) showed a decrease in radiance on day 21 (TMZ: 0.8; T-P: 0.55, 0.65, 0.94).

Supplementary Figure S5. Body weight changes of mice over time.

All tumor-bearing animals presented in Figure 8 were weighed on day 10 (start of daily treatment) and day 21 (48 hours after termination of treatment). Surviving animals were also weighed on days 29, 36, and 43. Shown is the average weight (grams) of all 8 animals in each treatment group. Circles: vehicle-treated; diamonds: TMZ-treated; triangles: T-P-treated. Arrow labeled Rx indicates the time period of treatment.

Supplementary Figure S6. Drug effects and body weight changes in mice.

D3H2LN cells were implanted into the brains of 16 nude mice. Ten days later, tumor take was confirmed via bioluminescent imaging, and treatment was initiated with vehicle only (control group; circles), 25 mg/kg POH (diamonds), 25 mg/kg TMZ (squares), or 25 mg/kg TMZ plus 25 mg/kg POH (triangles), once daily over the course of 10 days. (A) Kaplan-Meier survival plot of all animals carrying intracranial tumors. Arrow labeled Rx indicates the time period of treatment. Statistical difference between the groups of animals treated with TMZ vs. the combination of TMZ + POH: $p<0.41$ (i.e., not significant). (B) All animals were weighed on day 10 (start of daily treatment) and day 19 (end of treatment). Surviving animals were also weighed on day 28. Shown is the average weight (grams) of all 4 animals in each treatment group. Circles: vehicle-

treated; diamonds: POH-treated; squares: TMZ-treated; triangles: TMZ + POH-treated. Arrow labeled Rx indicates the time period of treatment.

Supplementary Table S1. Drug sensitivities of cells transfected with MGMT cDNA.

Cell Line	MGMT status	IC50 TMZ (μM)	IC50 T-P (μM)	Differential (-fold)
MDA-MB-231	—	9.9	2.3	4.3
231-MGMT-1	+	202	27	7.5
231-MGMT-2	+	212	34	6.2

Shown are IC50 values (i.e., drug concentrations that reduce colony forming ability by 50%) and differential toxicity between T-P and TMZ (i.e., fold increased potency of T-P over TMZ) in two MGMT-transfected clones in comparison to non-transfected parental cells.

Supplementary Figure S1

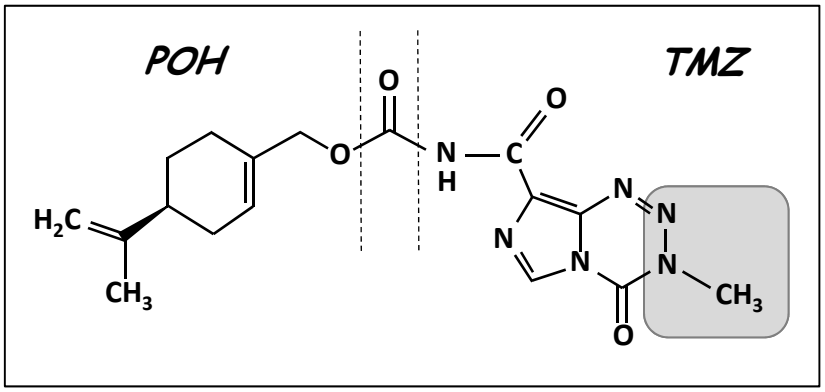

Supplementary Figure S2

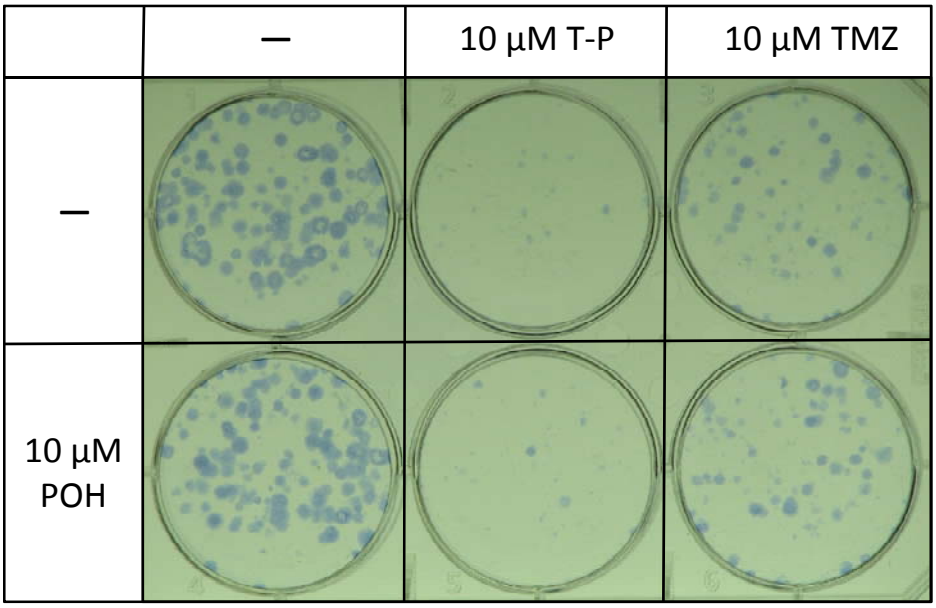

Supplementary Figure S3

A: Vehicle Treatment

intestine

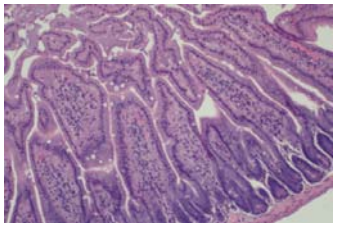

liver

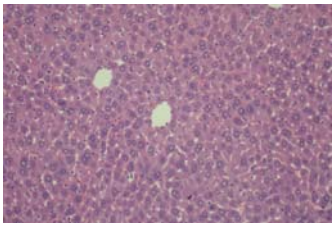

bone marrow

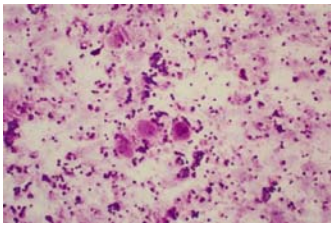

heart

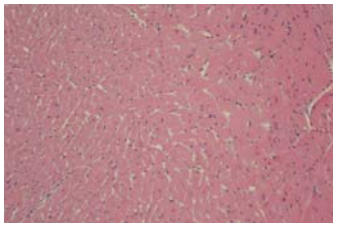

kidney

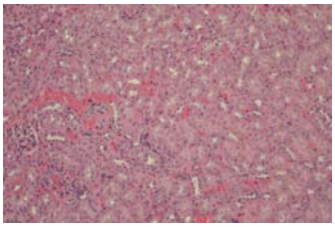

lung

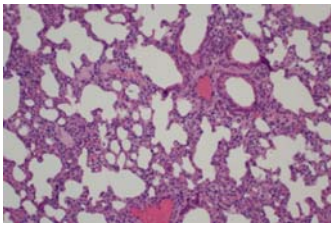

B: T-P Treatment

intestine

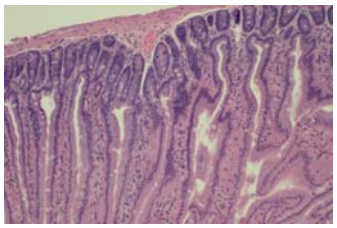

liver

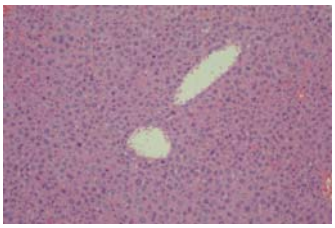

bone marrow

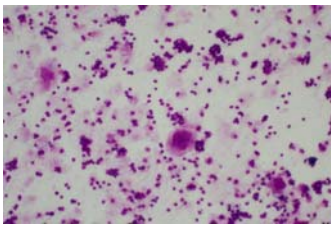

heart

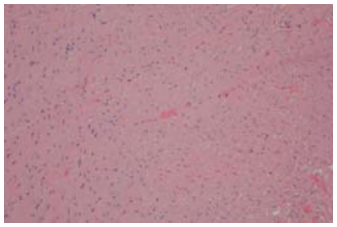

kidney

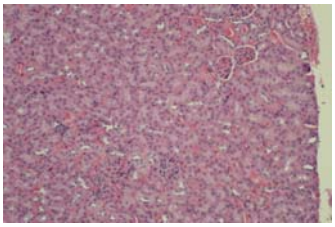

lung

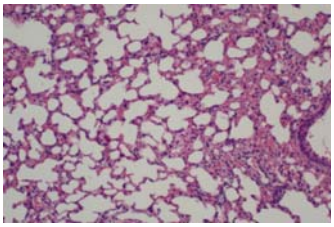

Supplementary Figure S4

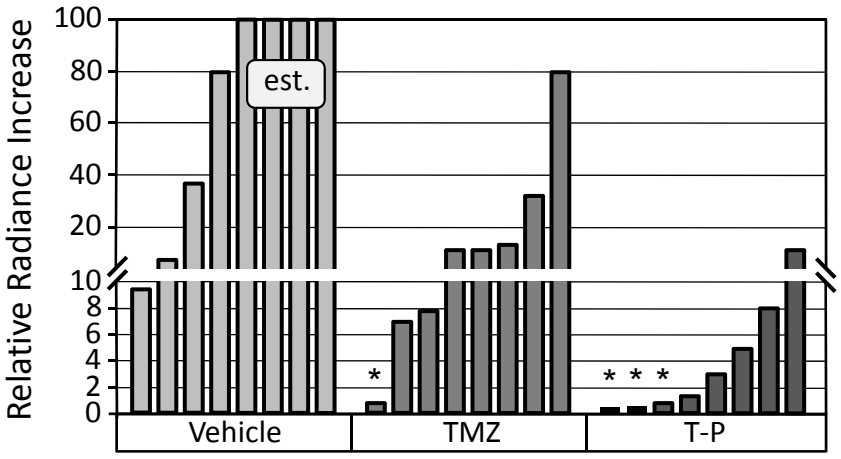

Supplementary Figure S5

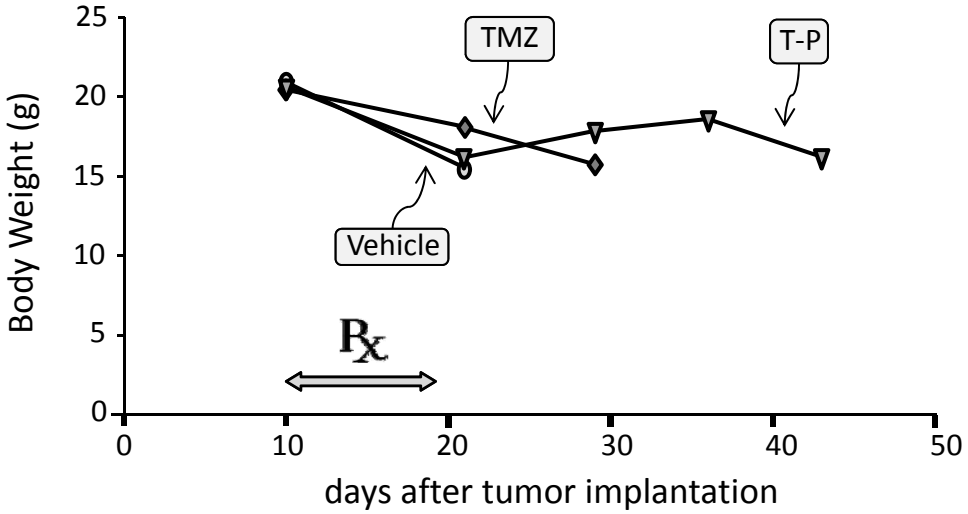

Supplementary Figure S6